Adsorption 11: 515–520, 2005

Compact Pressure Swing Adsorption Processes-Impact and Potential of New-Type Adsorbent-Polymer Monoliths

ANDREAS B. GORBACH*, MATTHIAS STEGMAIER AND GERHART EIGENBERGER
Institut für Chemische Verfahrenstechnik, Böblinger Straße 78, 70199 Stuttgart, Germany
gorbach@icvt.uni-stuttgart.de

JOCHEN HAMMER AND HANS-GERHARD FRITZ
Institut für Kunststofftechnologie, Böblinger Straße 70, 70199 Stuttgart, Germany

Abstract. The approach considered in this work is based upon the development of novel monolithic adsorbent-polymer materials, featuring low pressure drop and high mechanical stability. The potential is evaluated by comparison with commercial adsorbent pellets used in randomly packed beds. The adsorption of water vapor on a Zeolite 4A-Polyamide compound is considered as example case. Proper models for adsorption equilibrium and kinetics have been fit to measured data and implemented into a detailed PSA process model. This model has been validated by comparison with an experimental setup of a single column rapid PSA unit (RPSA). The productivity of the RPSA process has been analyzed for defined purity and recovery specifications and compared to a conventional design based on adsorbent pellets. The study shows that the novel adsorbent monoliths largely eliminate the kinetic and pressure drop limitations faced in conventional compact design, resulting in a substantial enhancement of productivity.

Keywords: RPSA, adsorbent, monolith, polymer

1. Introduction

Regarding the development of energetically efficient units for gas separation and gas purification, Pressure Swing Adsorption (PSA) processes offer a profitable approach (Ruthven et al., 1994). Particularly in small scale applications, like air drying or hydrogen purification and oxygen enrichment for mobile fuel cell systems, the compact design of the adsorber is crucial. To achieve the required high productivity, short cycle times must be applied (Rapid Pressure Swing Adsorption, RPSA). Hence small adsorbent particles must be used, providing sufficiently fast adsorption kinetics. However, high pressure drop and low mechanical stability (attrition) of the adsorbent are the limiting factors for particle size and thus process optimization. Consequently one can conclude that an economic operation of compact RPSA processes depends on the development of a more efficient mass transfer device.

Such mass transfer devices are used extensively as catalyst support in the form of monoliths. Monoliths combine short diffusion pathes (small channel wall thickness) with low pressure drop, thereby avoiding dusting, wall channeling and featuring easy modular design. The idea of using such monoliths in an adsorption process is not new, but relatively recent (Maclaine-Cross and Banks, 1972; Kodama et al., 1993; Li et al., 1998a). The significant difference to a catalytic process derives from the need of sorption capacity. The challenge comprises the manufacture of monolithic adsorbents that are not only coated but highly filled with the active component. However, if available, such devices augur well for the design of more compact processes with lower operating costs.

*To whom correspondence should be addressed.

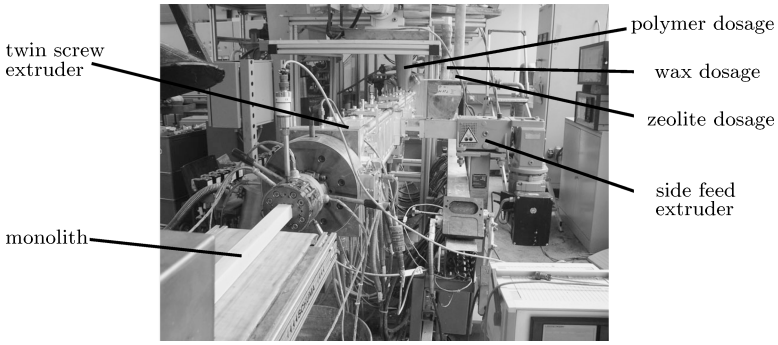

Figure 1. Manufacture of an adsorbent-polymer monolith by extrusion.

2. Manufacture

Monolithic adsorbents are so far usually made from ceramics (Otto et al., 1991; Li et al., 1998a, 1998b, 2000; Trefzger, 2002). Thereby the adsorbent (zeolite, silicatite), a hydrophilic plasticizing aid and an inorganic binder are mixed under high shear to form a uniform paste, which is then extruded. The emerging product has to be dried to expel water before it is calcinated at high temperatures to burn off organic contents and sinter the binder to enhance the strength. The resulting samples compare favorably with commercial pellets, equilibrium and kinetic properties are broadly the same. Indeed, the drying and firing programme is rather complex and often based on empiricism, making an automation difficult: it is crucial to control the weight loss, such that no bending or cracking occurs. Moreover, the high temperature during calcination results in a high energy demand.

The successful replacement of both organic plasticizing aid and inorganic binder with a polymer is the key issue of this work. The monoliths are manufactured by extrusion of polymer matrices highly filled with Zeolite powder using thermoplastic materials as plasticizing aid and binder (Hammer and Fritz, 2003; Fritz et al., 2003). Figure 1 shows the manufacturing setup. For the results shown in this manuscript, we used Polyamide (Ultramid A3SK, BASF, 17% mass fraction) as polymer and activated Zeolite 4A (SP565-10062, Grace, 70% mass fraction) as adsorbent. Both are fed to the extruder, which combines mixing and shaping of the compound. Since the product leaves the extruder dimensionally stable and contains no water, no drying or firing is necessary. Hence no rejects due to shrinking and cracking occur and energy-intensive high temperature treatment can be avoided.

However, an energy demand remains in order to generate a secondary pore structure. For this purpose a polymer wax (Licomont, Clariant, 13% mass fraction) is added to the above mixture as pore-forming agent. The after-treatment now consists of thermal wax extraction at moderate temperatures in an oven (210°C)[1]. The procedure is simple and easy to automate, keeping the potential costs for mass production low.

3. Characterization

Figure 2 depicts some typical monolith samples. Important properties are given in Table 1. The cell density

Table 1. Mechanical properties of some monolith samples.

	Mono1	Mono2	MonoC	SP7-9181
cpsi	100	200	400	–
D (cm)	1–3	1–3	1–3	–
s (mm)	0.8	0.5	0.3	–
ε_B	0.44	0.50	0.59	0.4
ϱ (g/cm^3)	1.15	1.15	1.15	1.13
R_m (N/mm^2)	≈30	≈30	≈30	≈30
FR	0.7–0.8	0.7–0.8	0.7–0.8	0.7–0.8

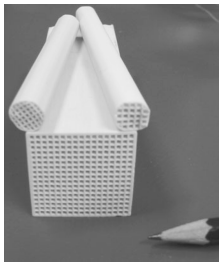

Figure 2. Adsorbent monoliths.

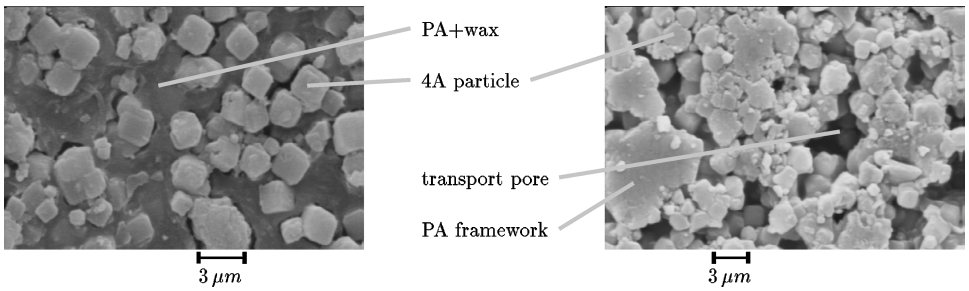

Figure 3. SEM images of a compound sample before (left) and after (right) the thermal after-treatment.

varies from 100 (Mono1) to 400 cpsi (MonoC), the channel wall thickness s from 0.8 to 0.3 mm respectively. The geometry can be either round or square with an outer diameter D in the range of 1–3 cm. In comparison to commercial granules (e.g. SP7-9181, Grace), the resulting bulk voidage ε_B is slightly higher. However, the material density ϱ, the compressive strength R_m and moreover the possible filling ratio with Zeolite FR are quite the same.

To obtain good mass transfer within the channel walls, it is important that the generated pore structure shows proper transport pores. Figure 3 shows SEM images of a compound sample before (left) and after the thermal after-treatment (right). It can be seen that the wax is removed, creating macropores ($<3\ \mu$m). The remaining polyamide (PA) framework ensures sufficient stability.

A quantification of the pore structure in comparison with a commercial pellet is given in Fig. 4, allowing for two important conclusions: The cumulative pore volume is about the same, whereas in agreement with earlier works (Li et al., 1998a) the monolith possesses a much higher macroporosity. Concerning the adsorptive properties this finding is very promising.

Using a static-volumetric operating principle, adsorption isotherms were obtained to investigate the capacity of the extrudates. As example case, the adsorption of water vapor on a Zeolite 4A-Polyamide compound (MonoC, cp. Table 1) is considered. The equilibrium data at four different temperatures is shown in Fig. 5. In agreement with the filling ratio, the capacity of the compound is approximately 80% of that of the pure Zeolite. Accordingly, the active adsorption centers are accessible and not blocked by the polymer. Furthermore, the typical shape of the Zeolite isotherm resembles well the shape of the equilibrium curve of the monolith. Thus it appears reasonable to model the isotherm of the monolith with an

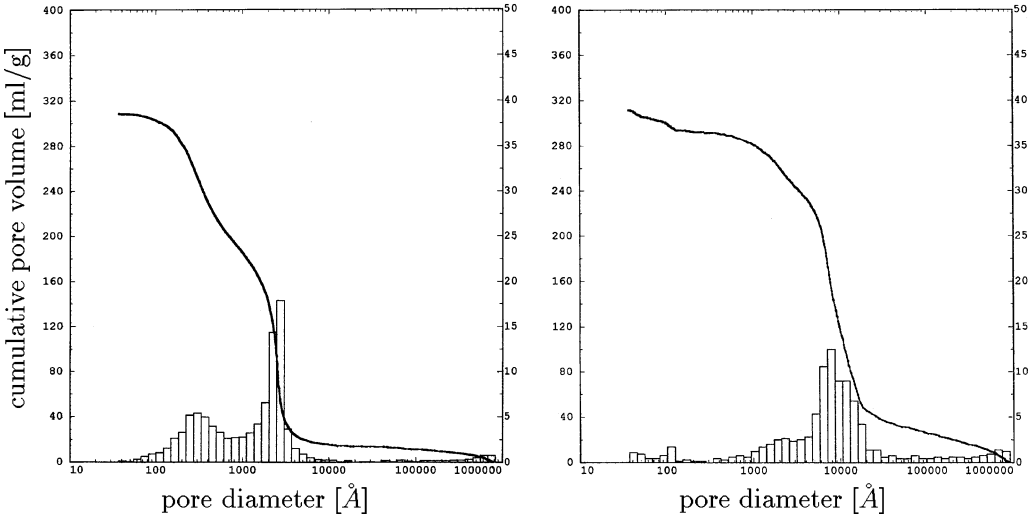

Figure 4. Pore size distribution of a commercial pellet (SP7-9181, left) and a monolith sample (MonoC, right).

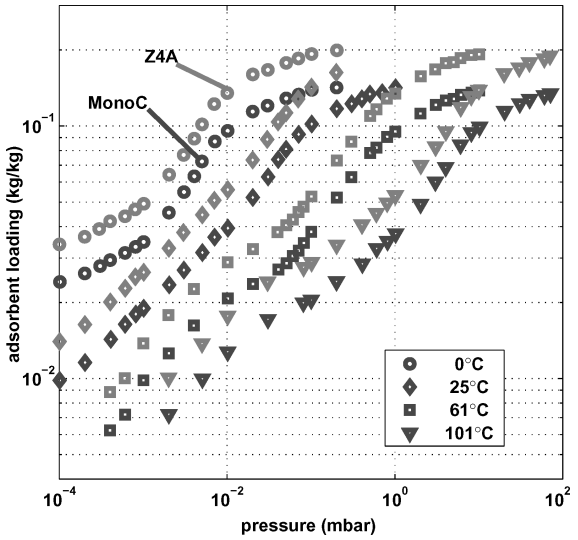

Figure 5. Equilibrium data of water vapor on Zeolite 4A (3μ-powder, SP565-10062) and a Zeolite 4A-Polyamide compound (MonoC, c.p. Table 1) at four different temperatures.

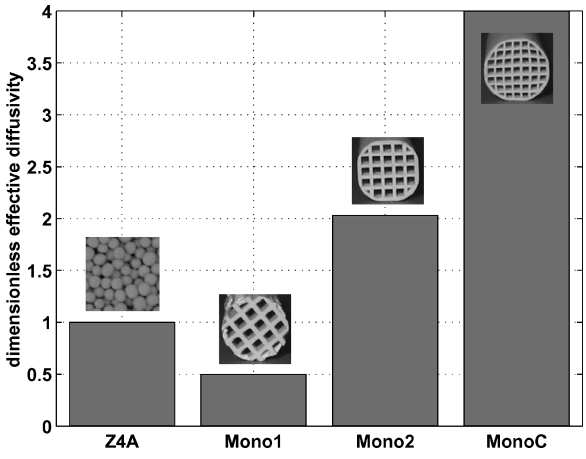

Figure 6. Dimensionless effective diffusivity of water vapor in three different monolith samples (cp. Table 1) normalized with the result of commercial granules Z4A (SP7-8374.518, 1.5 mm pellets).

appropriate model for the Zeolite. It has been shown that a good model fit over a range of six decades of partial pressure can be achieved with a rational class model with five temperature dependent parameters (Gorbach et al., 2004).

In order to determine the adsorption kinetics, a common dynamic breakthrough approach is used (Malek and Farooq, 1997). To derive information about the mass transfer coefficient, the profiles of the breakthrough experiments are matched with computer simulations. For the mass balance of the adsorbed amount of water, a modified linear driving force rate model is assumed, which has been developed for commercial 4A pellets. By identifying the dependency of the driving force on concentration, pressure and temperature, it is possible to accurately match the kinetics in a feasible range of operating conditions with only one state-invariant kinetic coefficient (Gorbach et al., 2004). Assuming isothermal operation, this effective mass transfer coefficient is the only remaining unknown and is used as adjustable fitting parameter. Figure 6 shows the result of this regression for three different monolith samples (cp. Table 1) normalized with the result of commercial granules Z4A (SP7-8374.518, 1.5 mm pellets). As expected, the mass transfer is enhanced by the shortening the diffusion path (channel wall thickness). The monolith with 400 cpsi provides a remarkable improvement of the kinetic coefficient by a factor of 4.

4. PSA Operation

To see how the aerodynamic and adsorptive properties of the monoliths affect the process performance, detailed computer simulations have been carried out. The underlying mathematical model is based upon previous work (Chihara and Suzuki, 1983; Ruthven et al., 1994). However, for adsorption equilibrium and kinetics the above mentioned models have been applied. Also, the Ergun momentum balance for packed beds is substituted with Poiseuille's equation.

Figure 7 depicts the RPSA performance of the monolith samples for constant recovery (50%). The corresponding operating conditions are given in Table 2. As expected, the productivity decreases with increasing product purity. Additionally, it can be observed how the productivity is enlarged by the shortening of the diffusion path, i.e. by the enlargement of the cell density, which is in good agreement with the according change of the mass transfer coefficient (cp. Fig. 6). These predictions are compared with results from an experimental unit of a single column RPSA, similar to setups presented elsewhere (Turnock and Kadlec, 1971; Jones et al., 1980). The experimental data reproduces well the qualitative characteristics of the performance, though partially differing by arround 50% due to the restricted accuracy of the measurement at very low water concentrations.

In comparison, Fig. 7 also displays the RPSA performance based on a packed bed which shows the same

Table 2. RPSA operating conditions.

D (cm)	T_p (s)	p_{ads} (bar)	p_{des} (bar)	T_{feed} ($^\circ C$)	N_{feed} (Nl/min)	y_{feed} (ppm)
3	10	5	1	25	10	1000

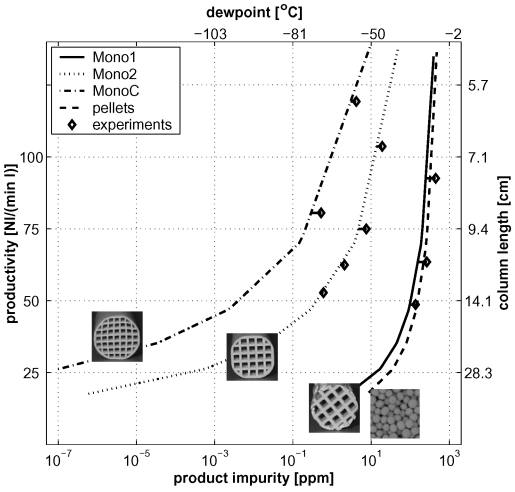

Figure 7. Simulated RPSA performance of the monolith samples for constant recovery (50%): experiments (diamonds) and simulations (lines). In comparison a packed bed with the same pressure drop as MonoC (dashed line).

pressure drop as the monolith MonoC. The resulting pellet diameter is about 3 mm and hence the adsorption kinetics become much slower: the respective kinetic coefficient differs by a factor of more than 15. In a quasi-isothermal process (low adsorptive concentration, rapid cycling) this change is almost proportional to the productivity. This is why the packed bed performance (dashed line) is even worse than that of the sample Mono1. The same conclusions can be deduced from Fig. 8. However, the picture now shows the productivity for constant product purity (-56°C dewpoint) and varying recovery. As can be seen, for low values of recovery, the productivity depends almost proportionally on its increase until an optimum is reached. Beyond this point, productivity drops rapidly as the recovery approaches the limit of minimal required flow rate (Skarstrom, 1972). As before, the difference in mass transfer affects directly the resulting productivity due to the respective change in the required bed length (for distinct recovery and purity). As a compromise, one can consider a packed bed with smaller pellets. Figure 8 displays this attempt for 1 mm granules. In fact, the productivity is clearly enlarged. However, this

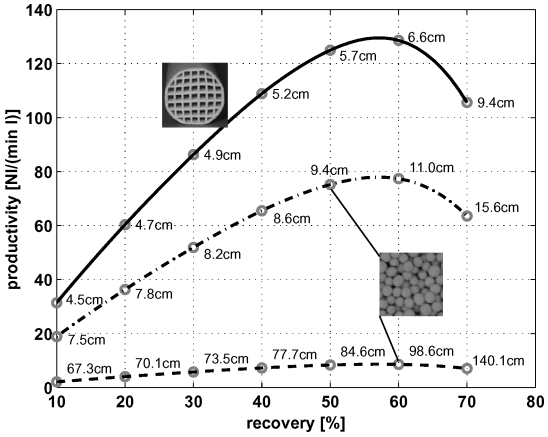

Figure 8. RPSA performance of monolith MonoC for constant product purity (-56°C dewpoint) vs. a packed bed with equal pressure drop (3 mm pellets, dashed line) and a packed bed with 1 mm pellets (dot-dashed line) with five times higher pressure drop. The corresponding bed lengths are indicated at distinct recoveries (circles).

enhancement is at the expense of a fivefold pressure drop.

5. Conclusions

In this contribution we presented a new approach for the manufacture of monolithic adsorbents with a thermoplastic polymer as plasticizing aid and binder. The manufacturing process is easy to automate, no rejects occur and the energy demand is lower than in conventional attempts. The resulting extrudates are mechanically stable, highly porous monoliths. Both adsorption equilibria and kinetics have been measured and modeled for the example case of water vapor adsorption on a Zeolite 4A compound. In comparison to commercial pellets, the adsorption capacity was found to be the same, whereas the mass transfer was clearly enhanced by the shortening of the diffusion path, yet featuring minor pressure drop. This improvement shifts the kinetic and aerodynamical limitations to higher productivities, allowing for more compact and efficient RPSA design. Future work shall be focused on the expansion of the procedure to bulk separation processes.

Nomenclature

cpsi	Cells per square inch
D	Outer monolith width (cm)
FR	Adsorbent filling ratio (−)

N_{feed}	Feed mole flow rate (Nl/min)
p_{ads}	Adsorption pressure (bar)
p_{des}	Desorption pressure (bar)
PA	Polyamide
PSA	Pressure Swing Adsorption
R_m	Compressive strength (N/mm^2)
RPSA	Rapid Pressure Swing Adsorption
s	Channel wall thickness (mm)
SEM	Scanning Electron Microscpoe
T_{feed}	Feed temperature (°C)
T_p	Total cycle time (s)
y_{feed}	Water feed mole fraction (−)
ε_B	Bulk void fraction (−)
ϱ	Compound density (g/cm^3)

Acknowledgements

The authors are grateful to the Deutsche Forschungsgemeinschaft for their financial support.

Note

1. This temperature is also the stability constraint for adsorbent activation. To guarantee zero loading, the monolith must either be packed in an activated state after extrusion or the activation must be enhanced by low pressure purging.

References

Chihara, K. and M. Suzuki, "Simulation of Nonisothermal Pressure Swing Adsorption," *J. Chem. Eng. Japan*, **16**(1), 53–61 (1983).

Fritz, H.G., J. Hammer, and H.H. Höfer, EP 200214666 (2003).

Gorbach, A., M. Stegmaier, and G. Eigenberger, "Measurement and Modeling of Water Vapor Adsorption on Zeolite 4A-Equilibria and Kinetics," *Adsorption*, **10** (2004).

Hammer, J. and H.-G. Fritz, "Entwicklung Zeolithischer Wabenkörper Mit Thermoplastischen Polymeren als Plastifizier- und Bindemittel," in "18. Stuttgarter Kunststoff-Kolloquium," 2003.

Jones, R., G. Keller, and R. Wells, "Rapid Pressure Swing Adsorption Process with High Enrichment Factor," U.S. Patent No. 4,194,892 (1980).

Kodama, A., M. Goto, and T. Hirose, "Experimental Study of Optimal Operation for a Honeycomb Adsorber operated with Thermal Swing," *J. Chem. Eng. Jap.*, **26**, 530–535 (1993).

Lee, L.Y., Perera, S.P., Crittenden, B.D. and Kolaczkowski, S.T., "Manufacture and Characterization of Silicalite Monoliths," *Adsorption Science & Technology*, **18** (2000).

Li, Y.Y., S.P. Perera, and B.D. Crittenden, "Zeolite Monoliths for Air Separation. Part 1: Manufacture and Characterization," *Chem. Eng. Res. Des.*, **76**(A8), 921–930 (1998a).

Li, Y.Y., S.P. Perera, and B.D. Crittenden, "Zeolite Monoliths for Air Separation. Part 2: Oxygen Enrichment, Pressure Drop and Pressurization," *Chem. Eng. Res. Des.*, **76**(A8), 931–941 (1998b).

Maclaine-Cross, I.L. and P.J. Banks, "Coupled Heat and Mass Transfer in Regenerators—Prediction Using Analogy with Heat Transfer," *Int. J. Heat Mass Transfer*, **15**, 1225–1242 (1972).

Malek, A. and S. Farooq, "Kinetics of Hydrocarbon Adsorption on Activated Carbon and Silica Gel," *AIChe Journal*, **43**(3), 761–776 (1997).

Otto, K., C.N. Montreuil, O. Todor, R.W. McCabe, and H.S. Gandhi, "Adsorption of Hydrocarbons and Other Exhaust Components on Silicalite," *Ind. Eng. Chem. Res.*, **30**, 2333–2340 (1991).

Ruthven, D.M., S. Farooq, and K.S. Knaebel, *Pressure Swing Adsorption*, VCH Publishers, New York, 1994.

Skarstrom, C.W., "Heatless Fractionation of Gases over Solid Adsorbents," *Heatless Fractionation of Gases over Solid Adsorbents,* pp. 95–106, CRC Press, Cleveland, 1972.

Trefzger, C., *Herstellung zeolithischer Wabenkörper*, Ph.D. thesis, Universität Stuttgart (2002).

Turnock, P.H. and R.H. Kadlec, "Separation of Nitrogen and Methane via Periodic Adsorption," *AIChE*, **17**(2), 335–342 (1971).